Charged pseudospin textures in double-layer quantum Hall systems: Bimerons and meron crystals

L. Brey
Instituto de Ciencia de Materiales (CSIC), Universidad Autónoma, 28049, Madrid, Spain

H. A. Fertig
Department of Physics, University of Kentucky, Lexington, Kentucky 40506-0055

R. Côté
Département de Physique, Université de Sherbrooke, Sherbrooke, Québec, Canada J1K 2R1

A. H. MacDonald
Department of Physics, Indiana University, Bloomington, Indiana 47405

(Received 26 June 1996)

Quasiparticle excitations of incompressible quantum Hall states at a total filling factor $\nu=1$ in a double-layer system have bimeron pseudospin textures. We studied the charge and pseudospin distributions and the energies of these quasiparticles as a function of layer separation, tunneling amplitude between the layers, and in-plane magnetic field strength by using a supercell microscopic unrestricted Hartree-Fock approach. We find that for typical double-layer system parameters, estimates of quasiparticle properties based wholly or partly on field-theoretic models require substantial quantitative revision. We comment on the nature of the crystal states expected at a finite but small quasiparticle density, and on limitations of the unrestricted Hartree-Fock approach. [S0163-1829(96)01248-9]

I. INTRODUCTION

Advances in semiconductor epitaxial growth techniques have led to the realization of double-quantum-well (DQW) systems with extremely high-mobility electron gases in nearby quantum wells. In some of these systems, the spacing between the two electron layers, d, is comparable to the typical electron spacing within a layer ($d\sim 100$ Å), and interesting effects can occur because of electronic correlation between electrons in different layers. This is especially true in the presence of a strong magnetic field B applied perpendicular to the electron layers. An interesting example is the occurrence, established by recent experimental[1] and theoretical[2,3] work, of spontaneous interlayer phase coherence in some incompressible quantum Hall effect (QHE) ground states.

In this work, we study charged excitations of the incompressible quantum Hall state at the total filling factor $\nu=1$. (Here $\nu\equiv N/N_\phi$ is the ratio of the number of electrons to the orbital degeneracy of a Landau level $N_\phi=AB/\Phi_0$, where A is the area of the system and Φ_0 is the magnetic flux quanta.) At $\nu=1$, it has been established[3] from several different theoretical points of view that, for sufficiently small separation between the layers, a broken symmetry can occur in which coherence exits between electrons in opposite layers in the absence of interlayer tunneling. This broken symmetry is favored by interlayer electron-electron interactions. The Hartree-Fock approximation for the broken symmetry ground-state wave function has the form[3]

$$|\Psi\rangle=\prod_X \frac{1}{\sqrt{2}}(C^+_{X,l}+e^{i\varphi}C^+_{X,r})|0\rangle. \qquad (1)$$

In this equation, X is a lowest Landau-level orbital label, $|0\rangle$ is the electron vacuum, and the operators $C^+_{X,l(r)}$ create an electron with the orbital quantum number X in the left (right) well. Since the product runs over all the possible values of X this state corresponds to filling factor $\nu=1$. By construction, this state has the same electronic charge in each layer, so that the electrostatic energy of the system is minimized when electric fields from external charges are balanced.[4] This state has long-range order in the phase difference between electrons in the two layers, φ. Since, in the absence of tunneling between the layers (t), the energy is independent of φ, the system has a continuous broken symmetry and will have a linearly dispersing Goldstone boson collective mode.

In the presence of tunneling, the energy is minimized when $\varphi=0$; in this case the many-particle wave function in Eq. (1) is composed of a full Landau level of single-particle orbitals which are symmetric combinations of the left and right layer orbitals. This wave function is evidently the exact ground state in the case of noninteracting electrons, and it is possible[3] to show that for $d\to 0$ it remains exact when interactions are included. For finite d, quantum fluctuations become important and the Hartree-Fock wave function is no longer exact. However, the broken symmetry ground state is expected[5,6] to survive for d smaller than a critical value d_c.

The quantum Hall effect is a low-temperature anomaly in the transport properties of double-layer systems in which the Hall resistance is accurately quantized and the dissipative resistance is $\propto\exp(-\Delta/2k_BT)$, where Δ is the charged excitation gap, i.e., it is the energy necessary to make excitations

with unbound charges. The quantum Hall effect occurs[7] when the chemical potential at $T=0$ has a discontinuity at a density which depends on magnetic field, most often at a fixed value of ν. The energy to add a particle to the system, μ^+, differs from the energy to remove a particle from the system, μ^-. If the excitations have charge e, as they do in the case of interest, $\Delta=\mu^+-\mu^-$ is equal to the chemical potential discontinuity associated with the incompressible state. The broken symmetry states discussed above are also incompressible states which exhibit the quantum Hall effect. At present, the property of these states which is most open to experimental study is Δ, which can be measured by studying the temperature dependence of the dissipative resistance at low temperatures, and which is expected to vanish for $d>d_c$. Indirect experimental evidence for the putative broken symmetry ground state in DQW systems has been obtained by studying the collapse of the QHE at $\nu=1$ at large layer separations.[8,9] The physics of the charge gap, Δ, at $\nu=1$ in double-layer systems, which is intimately connected with the broken symmetry ground state[3] at $t=0$, is the principle subject of this paper. One consequence of the spontaneous interlayer phase coherence in the DQW system at $\nu=1$ is the unusual sensitivity of Δ to the component of the magnetic field ($B_\parallel$) parallel to the layers.[10] Experimental studies have shown that the activation energy drops rapidly with increasing $B_\parallel$, until $B_\parallel$ reaches a critical strength ($B_{\parallel c}$) where a phase transition to a state whose activation gap is weakly dependent on $B_\parallel$ (Ref. 10) appears to occur. We will address the dependence of Δ on the hopping energy t and $B_\parallel$.

DQW system properties are conveniently described by mapping[6] the layer degree of freedom to an artificial pseudospin degree of freedom. In the $d=0$ case, a spinless DQW system is equivalent to a two-dimensional electron gas (2DEG) system with spin-$\frac{1}{2}$ particles and no Zeeman coupling. The 2DEG has SU(2) symmetry, and at $\nu=1$ the ground state is a strong ferromagnet[11] with total spin quantum number $S=N/2$. The mapping associates states in the left and right wells with the eigenstates of the σ_z Pauli spin matrix, so that the wave function in Eq. (1) is the $S=N/2$ state of a 2DEG at $\nu=1$, with the spins maximally aligned along the $[\cos(\varphi),\sin(\varphi),0]$ direction.

Two-dimensional ferromagnets in systems with SU(2) symmetry (Heisenberg ferromagnets) have topologically nontrivial *Skyrmion*[12] excitations. The experimental significance of these excitations in quantum Hall ferromagnets is magnified by the unique property[6,13] that topologically nontrivial spin-texture excitations carry an electrical charge.[6,13] In fact, these excitations can be and often are the lowest-energy charged excitations of $\nu=1$ quantum Hall ferromagnets, and therefore limit the activation energy Δ for dissipative transport processes. For Heisenberg quantum Hall ferromagnets, the lowest-energy charged excitations for zero Zeeman coupling are large Skyrmions, and Δ is half the Hartree-Fock quasiparticle gap.[13] For nonzero Zeeman coupling, the lowest-energy charged excitations are still usefully regarded as topologically charged spin textures, although the form and size of the charged-spin-texture excitations is determined by a complicated competition between the Hartree energy which favors extended charges and the Zeeman energy which favors small spin textures with a relatively small averaged number of reversed spins. (We follow the practice of the literature on quantum Hall ferromagnets and retain the Skyrmion label for these excitations as long as it is useful to regard them as charged spin textures.) For typical Zeeman coupling strengths, the energy gap Δ is only slightly smaller than the Hartree-Fock quasiparticle gap. However, the spin carried by the Skyrmions is much larger than for spin-$\frac{1}{2}$ charged excitations.[14–17] It is this difference in spin content which has made it possible to identify Skyrmion[18–20] excitations experimentally. For a finite Skyrmion density ($\nu\neq1$), the ground state is a square lattice Skyrme crystal.[21]

For $d\neq0$, the SU(2) symmetry of the 2DEG is reduced to U(1) symmetry because of the difference between interactions among electrons in the same layer and in different layers. The main effect is the appearance of a capacitive charging energy which locally favors equal density in the two layers. In the pseudospin language, this term favors configurations in which isospins are confined to the $\hat{x}$-$\hat{y}$ plane. The system maintains invariance under rotations about the $\hat{z}$ pseudospin axis, and behaves like an easy-plane XY ferromagnet rather than a Heisenberg ferromagnet. The change in the symmetry is responsible for a change in the dispersion of the Goldstone collective modes at long wavelengths[3] from quadratic to linear.[22] The change in the ground state from Heisenberg ferromagnet to easy-plane XY ferromagnet suggests that vortexlike spin textures might be important. Easy-plane ferromagnets have vortexlike spin-textures, called *merons*,[6] in which the order parameter tilts out of the easy plane in the vortex core. For quantum Hall ferromagnets, merons are pseudospin textures with charge $\pm e/2$.[6] Although the energy of an individual meron diverges logarithmically with the size of the system, two merons with like charge and opposite vorticities carry total charge $\pm e$ and have finite energy. We will call these charge $\pm e$ excitations *bimerons*. Meron pairs with opposite vorticities and opposite charges may lead to a Kosterliz-Thouless phase transition[6,23] in this system. The bimeron description[6,11,24,25] of the elementary charged excitations is appropriate only if the meron separation is large compared to the meron core size. For $d\rightarrow0$, as we discuss below, the bimeron evolves into a Skyrmion. In this limit, the meron pair description fails. Existing estimations of the bimeron excitation are based on microscopic calculations of the meron core energy and core size, but treat the interaction between merons[6,11,24,25] qualitatively.

The main purpose of this paper is to investigate the charged pseudospin-texture excitations of the DQW system. We describe their energy and size as a function of layer separation and the tunneling amplitude between the quantum wells. We find that although the bimeron picture often does apply qualitatively, it is not quantitatively reliable because of the relatively small separation between merons. We also study the effect that a parallel magnetic field has on charged pseudospin textures. We compare our results with previous descriptions of bimerons[6,11,24,25] which assume that the meron core is small compared to the optimal meron separation. We also discuss the ground state of the DQW system when the filling factor is slightly different from $\nu=1$, i.e., when a finite density of bimerons exists in the system.

The paper is organized as follows. In Sec. II, we review the long-wavelength effective Hamiltonian[6,11] which de-

scribes low-energy charged excitations of the $\nu=1$ DQW system, and discuss the picture of charged excitations which follows from this Hamiltonian. In Sec. III, we review predictions for charged-spin-texture excitations which follow from regarding bimerons as merons coupled only by the gradient term in the effective Hamiltonian.[6,11,24,25] In Sec. IV, we summarize the unrestricted Hartree-Fock method used for the present calculations. We present and discuss our numerical results, including results for the case of a finite density of charged spin textures, in Sec. V, and conclude in Sec. VI.

II. FIELD-THEORETICAL APPROACH

In a quantum Hall ferromagnet with Landau-level filling factor ν, spin textures and pseudospin textures which vary slowly on a microscopic length are accompanied by a charge density[6,13]

$$q(\mathbf{r})=-\frac{\nu}{8\pi}\epsilon_{\nu\mu}\mathbf{m}(\mathbf{r})\cdot[\partial_\nu\mathbf{m}(\mathbf{r})\times\partial_\mu\mathbf{m}(\mathbf{r})]. \tag{2}$$

This equation can be established[13] by assuming the quantization of the Hall conductivity and using the relationship between the Berry phase and the solid angle enclosed by the electronic spin orientation along a closed path. In Eq. (2), $q(\mathbf{r})$ is the charge density relative to the uniform density ferromagnetic ground state at filling factor ν, and $\mathbf{m}(\mathbf{r})$ is the unit-vector field which specifies the local direction of the pseudospin magnetic moment. The right-hand side of Eq. (2) is ν times the Pontryagian index density, or the topological charge density associated with the vector field $\mathbf{m}$.[12,26]

It follows from the relation between electrical and topological charge densities that the Hamiltonian describing low-energy excitations of the DQW system at $\nu=1$ must have the following form in the limit of slowly varying spin textures:[6]

$$\begin{aligned}H=&\frac{\rho_E}{2}\int d\mathbf{r}(\nabla m^\mu)^2+\tfrac{1}{2}\int d\mathbf{r}\,d\mathbf{r}'\,q(\mathbf{r})V(\mathbf{r}-\mathbf{r}')q(\mathbf{r}')\\&+\frac{\Delta_{\mathrm{SAS}}}{4\pi\ell^2}\int d\mathbf{r}(m_x(\mathbf{r})-1)+\beta\int d\mathbf{r}(m^z)^2\\&-\frac{e^2d^2}{16\pi\epsilon}\int\frac{d\mathbf{q}}{4\pi^2}qm^z_{-\mathbf{q}}m^z_{\mathbf{q}}+\frac{\rho_A-\rho_E}{2}\int d\mathbf{r}(\nabla m^z)^2.\end{aligned} \tag{3}$$

The first two terms of the Hamiltonian are SU(2) invariant contributions. The leading gradient term is the only term that appears in the nonlinear σ model (NLσM) for Heisenberg ferromagnets, and ρ_E is the spin stiffness in the x-y plane. The second term describes the SU(2) invariant Hartree energy corresponding to the charge density generated by Berry phases in quantum Hall ferromagnets. $V(\mathbf{r})$ is the Coulomb interaction screened by the dielectric constant ϵ of the host semiconductor. The third term describes the loss in tunneling energy when electrons are promoted from symmetric to antisymmetric states; here $\Delta_{\mathrm{SAS}}=2t$ is the single-particle splitting between symmetric and antisymmetric states. This term in the Hamiltonian of double-layer systems plays the same role as the Zeeman coupling in single-layer spin-$\frac{1}{2}$ systems. Here $\ell=(\hbar c/eB)^{1/2}$ is the magnetic length. The last three terms are the leading interaction anisotropy terms at long wavelengths. The $(\nabla m^z)^2$ term accounts for the anisotropy of the spin stiffness. Pseudospin order in the $\hat{x}$-$\hat{y}$ plane physically corresponds to interlayer phase coherence so that ρ_A-ρ_E will become larger with increasing d. The sum of the first and sixth terms in Eq. (3) gives an XY-like anisotropic nonlineal σ model (ANLσM). However, this gradient term is not the most important source of anisotropy at long wavelengths. The fourth term produces the leading anisotropy, and is basically the capacitive energy of the double-layer system.[27] The fifth term appears due to the long-range nature of the Coulomb interaction; its presence demonstrates that a naive gradient expansion of the anisotropic terms is not valid. ($m_{\mathbf{q}}$ is the Fourier transform of the unit vector field $\mathbf{m}$.) Equation (3) can be rigorously derived from the Hartree-Fock approximation in the limit of slowly varying spin textures,[6] and explicit expressions are obtained for ρ_E (which is due in this approximation entirely to interlayer interactions), ρ_A (due to intralayer interactions), and β. Quantum fluctuations will alter the values of these parameters from those implied by the Hartree-Fock theory.

If we retain only the first and last terms in Eq. (3), we have the ANLσM

$$H_0=\frac{\rho_E}{2}\int d\mathbf{r}(\nabla m^\mu)(\nabla m^\mu)+\frac{\rho_A-\rho_E}{2}\int d\mathbf{r}(\nabla m^z)^2. \tag{4}$$

The metastable spin-texture excitations of this model are identical to the analytically known metastable spin textures of the NLσM.[28,29,12] Because of the gradient terms in H_0, any finite-energy solution should approach a constant, $\mathbf{m}(\mathbf{r})\to\mathbf{m}_0$, when $|\mathbf{r}|\to\infty$. (Here $\mathbf{m}_0$ is any constant unit vector.) Consequently the 2D $\hat{x}$-$\hat{y}$ plane may be mapped to a unit sphere with all points at $|\vec{r}|\to\infty$ mapped to the south pole, and spin textures may be regarded as mappings[30] from the unit sphere to the unit sphere. Each finite-energy texture of the ANLσM is then characterized by an integer *winding number*, which is the number of times the first spherical surface *winds* the second one.

In the 2DEG problem, in the presence of an infinitesimal Zeeman coupling, the Skyrmion spin must point in the $\hat{z}$ direction for $|\vec{r}|\to\infty$. In the case of the DQW problem, however, even an infinitesimal capacitive term requires that $\hat{m}_0$ lie in the $\hat{x}$-$\hat{y}$ plane. A useful starting point for thinking about bimerons is to start from the ANLσM case. The resulting picture differs from that for single-layer 2DEG real spin Skyrmions only by this global rotation in pseudospin space. Each metastable state of the double-layer field theory classified by a topological number n consists of n pairs of merons with the same charge and different vorticities. We call these states nth-order bimerons. In particular, the $n=1$ solution is a simple bimeron, and the $n=-1$ solution a simple antibimeron. The winding number is equal to the topological charge,[12] and, due to the relation between the topological and real charge in our system, the bimerons are nontrivial quasiparticles excitations of the DQW $\nu=1$ incompressible ground state with charge e.

Following previous work,[12] it is convenient to parametrize the unit vector field $\mathbf{m}(\mathbf{r})$ in terms of the complex function w,

$$m_x + i m_y = \frac{2w}{1+|w|^2}. \tag{5}$$

In terms of w, the charge density has the expression

$$q(z) = \frac{1}{\pi} \frac{|\partial_z w|^2 - |\partial_{z*} w|^2}{(1+|w|^2)^2}. \tag{6}$$

(Here $z = x + iy$.) A general bimeron, which satisfies the requirement that its pseudospin texture lie in the x-y plane for $|\vec{r}| \to \infty$, is specified by a complex function of the form[28,29]

$$w(z) = \frac{z - z_L}{z - z_R} e^{i\varphi}, \tag{7}$$

where φ gives the azimuthal orientation of the projection of $\mathbf{m}$ in the x-y plane, at $|z| \to \infty$. The charge density of a bimeron is circularly symmetric around $|z_L + z_R|/2$, and its size is proportional to $|z_L - z_R|$. From m^z and $q(z)$, it is possible to obtain the charge density projected onto the left $[q_L(\mathbf{r})]$ and right $[q_R(\mathbf{r})]$ wells. $q_L(\mathbf{r})$ and $q_R(\mathbf{r})$ have maxima at z_L and z_R, respectively. In a *naive* picture, z_L and z_R are the centers of the two merons which form the bimeron. It should be noted that $q_{L(R)}(\mathbf{r})$ are not symmetric around $z_{L(R)}$. In the ANLσM, the energy of a neutral bimeron or antibimeron is $E^0_{\rm bm} = (4\pi/3)(2\rho_E + \rho_A)$. In the $d = 0$ case, the cost in energy of creating a bimeron-antibimeron pair is one-half the energy cost of creating a single-particle electron-hole pair.[13] When a finite Zeeman term is present, a microscopic description of the problem shows that the energy difference is reduced, but the spin textures still have a lower energy than single-particle electron-hole pairs.[14] In this work, we confirm that this is also the case for finite values of the layer separation d.

Now we describe qualitatively the effect that the other terms of the low-energy Hamiltonian Eq. (3) have on the solution of the ANLσM. The second term in Eq. (3) is the SU(2) invariant part of the Hartree energy which favors infinity large bimerons. In the case of $\Delta_{\rm SAS} = 0$, the terms in Eq. (3) which favors finite-size bimerons are the fourth and fifth ones. This term is a dipolar contribution which appears due to the long-range character of the Coulomb interaction. Tunneling plays the same role as the Zeeman energy in the 2DEG, favoring a finite-size quasiparticle.[14] These terms also change the functional form of the bimeron. In order to obtain the actual form and energy of the charged pseudospin textures, it would be necessary to minimize the Hamiltonian (3). However, the addition of the extra terms to the simplest Hamiltonian H_0 tends to favor small size bimerons, which are often not correctly described by the Hamiltonian (3), which is only valid in the limit of slowly varying spin textures. In order to describe charged pseudospin textures of any size, we use a microscopic Hartree-Fock (HF) approximation which has previously been successfully used for describing spin textures in the 2DEG system at $\nu = 1$.[14,21]

III. SPIN-TEXTURE QUASIPARTICLES IN COHERENT DOUBLE-LAYER SYSTEMS

In this section, we will review some of the physical pictures and quantitative estimates for charged-spin-texture excitations in coherent double-layer quantum Hall systems which have been developed by previous workers using a field theory approach. These pictures and estimates will be compared with Hartree-Fock results in Sec. V. Previous works on charged pseudospin textures in DQW's treat them as if composed of two charge $e/2$ merons with opposite vorticities.[6,11,24,25] In this section, we briefly review the results obtained with this approximation.

A. No tunneling between layers

Due to the gradient terms in the effective Hamiltonian of Eq. (3), the energy of an *isolated* meron with charge $\pm e/2$, can be written in the form

$$E^{\pm}_m = E^{\pm}_{\rm mc} + \pi \rho_E \ln R/R_{\rm mc}; \tag{8}$$

here $E^{\pm}_{\rm mc}$ are the meron-core energies, and $R_{\rm mc}$ is the meron-core radius. The size of the meron does not depend on the sign of the charge. The quantities $R_{\rm mc}$ and $E^{\pm}_{\rm mc}$ do not depend on the vorticity, but on the distance between wells. The logarithmic term appears because the meron has a topological charge $\pm 1/2$. The meron charge density has circular symmetry around the meron center.

In order to cancel the logarithmic divergence and obtain finite-energy charged excitations, it is necessary to combine two merons with opposite vorticities. In this case, it is necessary to take into account the Hartree repulsion between merons with the same charge $e/2$. The repulsion appears because of the equivalence between topological and real charge. Including the Hartree repulsion, the energy of two merons separated by a distance R is

$$E^{\pm}_{\rm mp} = 2E^{\pm}_{\rm mc} + \frac{e^2}{4\epsilon R} + 2\pi\rho_E \ln(R/R_{\rm mc}). \tag{9}$$

The equilibrium distance between merons, R^*, and meron-pair energy are obtained by minimizing $E^{\pm}_{\rm mp}$ with respect to R.

This approach for the meron pair energy is valid provided R^* is larger than $R_{\rm mc}$. Using HF estimations for $\rho_E, R_{\rm mc}$, and $E^{\pm}_{\rm mc}$, Yang and MacDonald[25] obtained $E^{\pm}_{\rm mp}, R_{\rm mc}$, and R^*. They found that $R_{\rm mc}$ decreased continuously with d, and that R^* increases with d. At a layer separation $d \sim 0.5\ell$, $R^* = R_{mc}$, and they concluded[25] that their estimates would be reliable in the range $0.5\ell < d < d_c$. In this range, the charge gap in the system, $E^{+}_{\rm mp} + E^{-}_{\rm mp}$, is almost one-half the HF single-particle gap, in approximate agreement with exact diagonalization studies.[6]

B. Tunneling amplitude different from zero

The effect of the tunneling on the charged pseudospin texture energy has been also estimated.[24,11] When $t \neq 0$, the U(1) symmetry in the problem is destroyed and the pseudospin must point in the $\hat{x}$ direction for $|\vec{r}| \to \infty$. As $\Delta_{\rm SAS} = 2t$ increases, the bimeron configuration gradually transforms into a pseudospin configuration with a domain wall connecting the meron cores.[31] The string tension of the domain wall is

$$T_0 = \frac{8\rho_E}{\xi}, \tag{10}$$

where

$$\xi=\left[\frac{4\pi\ell^2\rho_E}{\Delta_{\rm SAS}}\right]^{1/2} \tag{11}$$

is the width of the domain wall. Assuming that the distance between merons, R, is much larger than ξ, the energy of the positive charged meron pair in this limit can be written as

$$E'_{\rm mp}=2E'_{\rm mc}+\frac{e^2}{4\epsilon R}+T_0R. \tag{12}$$

The prime in $E'_{\rm mc}$ is included to emphasize that $E_{\rm mc}$ will depend on $\Delta_{\rm SAS}$. The meron-pair energy is minimized at $R'_0=\sqrt{e^2/4\epsilon T_0}$, and takes the value $2E'_{\rm mc}+\sqrt{e^2T_0/\epsilon}$. Note that, apart from the variation of the meron-core energy with $\Delta_{\rm SAS}$, the meron-pair energy varies as $\Delta_{\rm SAS}^{1/4}$, in contrast to the case of single-particle excitations where the gap changes linearly with $\Delta_{\rm SAS}$. This picture applies for $\xi<R'_0<R^*$. In Ref. 11, it is estimated that the crossover from the meron-pair picture to the finite-length domain-wall picture of the charged quasiparticle occurs for $\Delta_{\rm SAS}/(e^2/\epsilon\ell)\sim 8\times 10^3[\rho_E/(e^2/\epsilon\ell)]^3$. This estimate, combined with the HF estimate of ρ_E, suggests that the domain-wall picture will apply except for samples prepared to make $\Delta_{\rm SAS}$ as small as possible. Note also that for large values of $\Delta_{\rm SAS}$, R'_0 decreases and for $R'_0\sim\ell$, the meron-pair description cannot apply.

C. Effect of a parallel magnetic field

A finite component of the magnetic field ($B_\parallel$) in the $\hat{y}$ direction, induces a position-dependent phase in the tunneling amplitude $t\rightarrow te^{iQx}$, where $Q=d/\ell^2$ and $\ell_\parallel=\sqrt{\hbar c/eB_\parallel}$ is the magnetic length corresponding to $B_\parallel$. In the pseudospin language tunneling maps to a fictitious magnetic field $\mathbf{h}(\mathbf{r})=t(\cos Qx,\sin Qx,0)$, which has a Zeeman coupling with the pseudospin unit vector field $\mathbf{m}(\mathbf{r})$. Two terms are important in the Hamiltonian in order to describe the ground state at $\nu=1$: a tunneling term which favors a pseudospin texture aligned locally with the rotating Zeeman field $\mathbf{h}(\mathbf{r})$, and a gradient term representing the energy cost associated with the spatial variation of $\mathbf{m}(\mathbf{r})$. Neglecting the pseudospin component in the z direction, the effective Hamiltonian at $\nu=1$ can be written

$$H=\int d\mathbf{r}\left[\frac{1}{2}\rho_E|\nabla\varphi|^2-\frac{\Delta_{\rm SAS}}{4\pi\ell^2}\cos(\varphi(\mathbf{r})-Qx)\right], \tag{13}$$

where $\varphi=\arctan(m_y/m_x)$. For small Q and/or small ρ_E, the phase obeys $\varphi(\mathbf{r})=Qx$, and the order parameter rotates *commensurately* with $\mathbf{h}(\mathbf{r})$. At larger $B_\parallel$, $\mathbf{h}(\mathbf{r})$ rotates too rapidly, and a phase transition to a soliton lattice occurs. The critical value of Q where the phase transition from the commensurate phase to the soliton phase occurs is[23,32]

$$Q^*\ell=\left(\frac{2}{\pi}\right)^{3/2}\left(\frac{\Delta_{\rm SAS}}{2\rho_E}\right)^{1/2}. \tag{14}$$

At Q^*, the commensurate phase is destroyed by the creation of walls separating domains where the pseudospin is constant. In each domain wall, the pseudospin phase slips by 2π relative to the rotating Zeeman field. These domain walls are the solitons which appears as solution of Eq. (13). At larger Q, the distance between the solitons becomes of the same order as the soliton width, and the soliton lattice phase asymptotically approaches an *incommensurate* phase where: $\varphi\sim$ const. From Eq. (13), the incommensurate phase has lower energy than the commensurate phase at $Q_{C\rightarrow I}=\sqrt{\Delta_{\rm SAS}/2\pi\rho_E}$.

In this paper, we attempt to address the question of how the charge gap of the DQW system at $\nu=1$ changes with $B_\parallel$. When $B_\parallel=0$, the direction of the string joining the merons is arbitrary. The first effect of having $B_\parallel\neq 0$ is to define a preferred direction in the system: in order to lower the gradient energy, the domain walls will want to line up in the y direction.[24,11] The second effect is a reduction in the string tension. In the commensurate phase, the effective string tension is[24,11]

$$T=T_0\left[1-\left(\frac{Q}{Q^*}\right)^2\right]. \tag{15}$$

The meron-pair energy is minimized at a distance between merons, $R''_0=\sqrt{e^2/4\epsilon T}$, and the energy of the positively charged meron pair, far in the commensurate phase, is

$$2E^+_{\rm mc}+\left(\frac{e^2T_0}{\epsilon}\right)^{1/2}\left[1-\left(\frac{Q}{Q^*}\right)^2\right]^{1/2}. \tag{16}$$

Observe that there is a large reduction in the charge gap when Q increases. Read[24] studied the behavior of the charge gap for all ranges of $B_\parallel$ more thoroughly. He found that, because of the vanishing string tension at the transition to the soliton lattice state, there should be a symmetric square-root singularity in the gap for Q near Q^*.

The attractive physical pictures developed above assume that the meron-core size is small compared to the string length, and this is small compared to the meron-pair separation in the absence of tunneling. Correspondingly the internal structure of the meron is assumed to play a negligible role in the energetics. Our objective below in comparing with microscopic Hartree-Fock results is to help determine when these assumptions do apply, and to see what aspects of these physical pictures survive when the meron cores become large and polarizable.

IV. METHOD OF CALCULATION

We now turn our attention to microscopic calculations, which free us from assumptions about the meron core and domain-wall sizes and enable us to include all relevant contributions to the quasiparticle energy. As explained in Sec. III, the size and form of bimeron pseudospin-texture quasiparticles is determined by competition between gradient, Hartree, and tunneling energies. Since these three terms are well described by the HF approximation, we expect that this mean-field approach should give an accurate description of charged excitations in DQW systems. We also know that in the case of the 2DEG the HF approximation gives extremely accurate results for spin-texture quasiparticles.[14].

For the single-layer 2DEG with spin, the Hartree-Fock approximation for a microscopic Skyrmion-like charged-spin-texture state centered on the origin has single-particle

orbitals in which the angular momentum of the up-spin differs from the angular momentum of the down-spin by a single unit. This mixing produces an azimuthal spin-texture component which winds by 2π around a circle centered on the origin, and results in self-consistent-field equations[14] which require only 2×2 matrices[14] to be diagonalized. In the DQW case, the lack of circular symmetry in a bimeron state leads to Hartree-Fock self-consistent-field equations which do not decouple, and the resulting numerical calculation would be more difficult. We avoided this complication by considering a crystal of identical bimerons, and taking the limit of large lattice constants. Although the bimerons interact by means of the long-range Coulomb interaction, it is usually possible to extract properties of isolated bimerons from these crystal calculations. At the same time, we are able to obtain results for the crystal states which presumably occur for a low but finite density of bimerons.

Since we are essentially dealing with a strong field phenomenon, and we are interested in states for which the tunneling gap is much smaller than the cyclotron gap, we will only consider states in the lowest Landau level. In the Landau gauge, the single-particle states are given by

$$\psi_{X,j}(\mathbf{r})=\frac{1}{\sqrt{L_y \ell \pi^{1/2}}} e^{iXy/\ell^2} e^{-(x-X)^2/2\ell^2} \chi_j(z). \quad (17)$$

Here X is the electron guiding center, and $\chi_j(z)$ with $j=R,L$ is the envelope wave function of the lowest-energy state centered in the right or left well. It is convenient to define the operators

$$\rho_{j,j'}(\mathbf{q})=\frac{1}{N_\phi}\sum_{X,X'} e^{-(i/2)q_x(X+X')}\delta_{X,X'-q_y\ell^2} C^+_{X,j} C_{X',j'}, \quad (18)$$

so that the Fourier transform of the density operator can be written as

$$n(\mathbf{q},z)=N_\phi \sum_{j,j'} e^{-(q^2\ell^2/4)} \chi^*_j(z)\chi_{j'}(z)\rho_{j,j'}(\mathbf{q}). \quad (19)$$

The HF mean-field Hamiltonian of the DQW system is therefore

$$H_{\mathrm{HF}}=-N_\phi \frac{\Delta_{\mathrm{SAS}}}{2}[\rho_{L,R}(0)-\rho_{R,L}(0)] + N_\phi \frac{e^2}{\epsilon \ell}\sum_{\mathbf{q},i,j} V_{i,j}(\mathbf{q})\rho_{i,j}(\mathbf{q}), \quad (20)$$

where

$$V_{L,L}=[V_a(q)-V_b(q)]\langle\rho_{L,L}(-\mathbf{q})\rangle+V_c(q)\langle\rho_{R,R}(-\mathbf{q})\rangle,$$

$$V_{R,R}=[V_a(q)-V_b(q)]\langle\rho_{R,R}(-\mathbf{q})\rangle+V_c(q)\langle\rho_{L,L}(-\mathbf{q})\rangle, \quad (21)$$

$$V_{i,j}=-V_d(q)\langle\rho_{j,i}(-\mathbf{q})\rangle, \quad i\neq j.$$

In Eq. (21),

$$V_a(q)=\frac{e^{-q^2\ell^2/2}}{q\ell},$$

$$V_b(q)=\int_0^\infty d(q'\ell) J_0(qq'\ell^2) e^{-(q'^2\ell^2/2)},$$

$$V_c(q)=\frac{e^{-q^2\ell^2/2}}{q\ell} e^{-qd}, \quad (22)$$

$$V_d(q)=\int_0^\infty d(q'\ell) J_0(qq'\ell^2) e^{-(q'^2\ell^2/2)} e^{-qd},$$

and J_0 a Bessel function of the first kind.

In order to obtain the HF solutions at a given ν, we solve Eqs. (20) and (21) self-consistently using the one-electron Green's-function equation-of-motion approach.[5]

Hamiltonian (21) has a number of different solutions corresponding to different states of the DQW system. Each of these solutions is characterized by a set of order parameters $\langle\rho_{i,j}(\mathbf{G})\rangle$, where the wave vectors $\mathbf{G}$ are the reciprocal-lattice vectors of the periodic structure considered. To enforce a particular solution, we start in the first iteration of Eqs. (20) and (21) with a set of parameters $\langle\rho_{i,j}(\mathbf{G})\rangle$ with the desired translational and pseudospin texture symmetries.

Given a symmetry, we have to find the minimum energy solution of the HF Hamiltonian. The HF total energy has the expression

$$E_{\mathrm{HF}}=\langle H_{\mathrm{HF}}\rangle-\tfrac{1}{2}N_\phi \frac{e^2}{\epsilon\ell}\sum_{\mathbf{q},i,j} V_{i,j}(\mathbf{q})\rho_{i,j}(\mathbf{q}). \quad (23)$$

The energy per electron is simply $E=E_{\mathrm{HF}}/N$.

To study isolated bimerons, we solve Eqs. (20) and (21) self-consistently for filling factors close to $\nu=1$. In the very dilute limit, $\nu\to 1$, we extract information corresponding to isolated bimerons from our results. We look for periodic structures with one extra electron per unit cell with respect to $\nu=1$, i.e., a single bimeron per unit cell. In this limit of almost independent bimerons, the results obtained for quasiparticles on triangular and square lattices are nearly identical. In the square lattice case, the lattice parameter for a given filling factor ν is $\sqrt{2\pi/|1-\nu|}$, and the quasiparticle interaction effects can be approximated by the point-particle Madelung energies of the lattices, and these are usually much smaller than the relevant energies in the problem.

We express our results for the quasiparticle energies in terms of the energy ($\varepsilon_{\mathrm{qp}}$) increase per quasiparticle, when the quasiparticles $N_{\mathrm{qp}}=|N-N_\phi|$ are created at fixed number of electrons by varying N_ϕ:

$$\varepsilon^{\pm}_{\mathrm{qp}}=\frac{\nu}{|1-\nu|}[E-\varepsilon_0(d)]; \quad (24)$$

the plus sign corresponds to the bimeron case ($\nu>1$), and the minus to the antibimeron case ($\nu<1$). $\varepsilon_0(d)$ is the energy per electron at the $\nu=1$ incompressible state,

$$\varepsilon_0(d)=-t-\tfrac{1}{4}[V_b(q=0)+V_d(q=0)]. \quad (25)$$

In the limit of vanishing bimeron density ($\nu \to 1$), the quantity $\varepsilon_{\rm qp}^{\pm}$ is the so-called neutral quasiparticle energy,[33,34] related to the chemical potentials $\mu^{\pm}$ at densities just larger and just smaller than the critical density at $\nu=1$, through the relation

$$\mu^{\pm} = \pm \varepsilon_{\rm qp}^{\pm} + \varepsilon_0(d). \tag{26}$$

As a consequence of the particle-hole symmetry which applies in the thermodynamic limit, the chemical potential satisfies the relation

$$\mu^{+} + \mu^{-} = 2[\varepsilon_0(d=0) + t]. \tag{27}$$

It is therefore possible to extract the charge gap of the system from the knowledge of $\varepsilon_{\rm qp}^{+}$ alone:

$$\Delta = \mu^{+} - \mu^{-} = 2\varepsilon_{\rm qp}^{+} + 2[\varepsilon_0(d) - \varepsilon_0(d=0)]. \tag{28}$$

It is useful to consider the quasiparticle energy as the sum of Hartree, exchange, and tunneling energy contributions. These contributions to $\varepsilon_{\rm qp}^{\pm}$ are given by terms of corresponding origin on the right-hand side of Eq. (24). When the size of the bimerons is much smaller than the distance between bimerons, the Hartree energy is reduced, in our calculations, by the Madelung energy per quasiparticle.[35] In the triangular lattice, $\varepsilon_{\rm MAD} \simeq -0.7821|1-\nu|^{1/2} e^2/\epsilon\ell$. In the dilute limit, this is the dominant interaction contribution to $\varepsilon_{\rm qp}^{\pm}$, and we subtract this contribution from our numerical results. The tunneling term is proportional to the one-electron tunneling gap $\Delta_{\rm SAS}$. The constant of proportionality is $\langle S \rangle$, the mean number of electrons in antisymmetric states. This quantity provides a measure of the size of the quasiparticles; for single-particle excitations, $\langle S \rangle = 1$.

Once the HF equations have been solved self-consistently the charge and spin densities can be evaluated from the following expressions. The charge density is (A is the area of the system)

$$n(\mathbf{r}) = \frac{N_\phi}{A} \sum_{\mathbf{G}} \left[\langle \rho_{L,L}(\mathbf{G}) \rangle + \langle \rho_{R,R}(\mathbf{G}) \rangle \right] e^{-G^2\ell^2/4} e^{-i\mathbf{G}\cdot\mathbf{r}}. \tag{29}$$

Components of the pseudospin density are given by

$$S_z(\mathbf{r}) = \frac{N_\phi}{2A} \sum_{\mathbf{G}} \left[\langle \rho_{L,L}(\mathbf{G}) \rangle - \langle \rho_{R,R}(\mathbf{G}) \rangle \right] e^{-G^2\ell^2/4} e^{-i\mathbf{G}\cdot\mathbf{r}},$$

$$S_x(\mathbf{r}) + iS_y(\mathbf{r}) = \frac{N_\phi}{A} \sum_{\mathbf{G}} \langle \rho_{L,R}(\mathbf{G}) \rangle e^{-G^2\ell^2/4} e^{-i\mathbf{G}\cdot\mathbf{r}}. \tag{30}$$

V. NUMERICAL RESULTS

For a given translational symmetry, we solve Eqs. (20) and (21) self-consistently for a set of order parameters, $\langle \rho_{i,j}(\mathbf{G}) \rangle$. We include reciprocal-lattice vectors with $|\mathbf{G}| < G_{\rm max}$, and increase $G_{\rm max}$ until our numerical results converge. Since the number of reciprocal-lattice vectors needed to obtain accurate results increases rapidly with the size of the unit cell, our approach fails if the bimeron lattice is too dilute. We are generally able to obtain accurate results only for $|\nu - 1| > 0.01$.

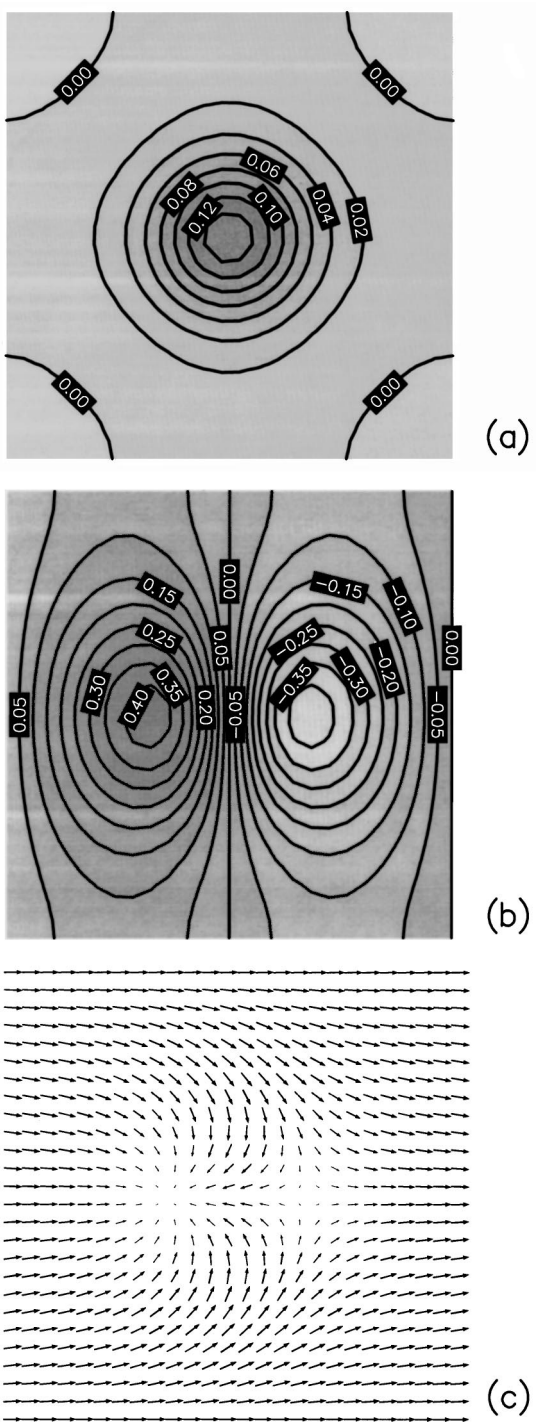

FIG. 1. (a) Excess of total charge density with respect to the filling factor $\nu=1$, $n(\mathbf{r}) - 1/(2\pi\ell^2)$. (b) z component of the pseudospin density $S_z(\mathbf{r})$. (c) Two-dimensional vector representation of the x-y components of the pseudospin density for a quasiparticle in the cases $\nu = 1.02, d=0$, and $t=0$. The figure corresponds to a square unit cell. In (a) and (b), the numerical values are given in units of $1/2\pi\ell^2$. In (c), the length of the arrows is proportional to the local magnitude of S_x and S_y, and their direction indicates the local orientation.

A. No tunneling between layers

In Fig. 1, we plot, for the case where $d=0$ and $t=0$, (a) the total charge density $n(\mathbf{r})$, (b) the z component of the pseudospin density $S_z(\mathbf{r})$, and (c) the two-dimensional vec-

tor representation of the x-y components of the pseudospin density. The figure corresponds to the unit cell used in the calculations. These results have been obtained using a square lattice, with a single quasiparticle per unit cell, and a filling factor $\nu=1.02$, i.e., the distance between the quasiparticles is $\sim 18\ell$. Because $d=0$, the system has SU(2) symmetry and the quasiparticles are Skyrmions. The total charge density has nearly circular symmetry around the Skyrmion center. In the $d=0$ and $t=0$ case, the only nonzero terms in Eq. (3) are the gradient and Hartree terms, and a single Skyrmion would have unlimited size. In our calculation, the Skyrmions have finite size solely as a result of repulsive interactions with their neighbors. This conclusion will be more evident when we show the dependence of the quasiparticle size with filling factor.

In Fig. 1, we also plot the Skyrmion spin density. Note that the spin texture is well described by Eq. (7), with $z_L=(-3.2,0), z_R=(3.2,0)$, and $\varphi=0$ (the origin is the center of the unit cell). It is important to note that the results shown in Fig. 1 are nearly identical to those for a NLσ model Skyrmion, and the main difference in comparison with familiar plots for the single-layer case is just a global rotation of the spin field. Also note that the charge density contributions from left and right quantum wells are not circularly symmetric around $z_L(z_R)$ or around the origin. The electron density projected in the left (right) *well* has a maximum at z_L (z_R) and a minimum at $z_R(z_L)$, also in agreement with the Skyrmion shape given by Eqs. (5)–(7).

When the distance between wells increases, the charge density shape gradually changes; as d increases it assumes an approximately ellipsoidal form while at large values of d $(d>0.6\ell)$ separate maxima centered at z_L and z_R appear. In Fig. 2, we show the same quantities as in Fig. 1 but for the case $d=0.8\ell$. Note that in this case the form of the solution is still reasonably approximated by Eqs. (5)–(7). Now the distance between the merons is smaller, $z_L=(-1.8,0.0)$ and $z_R=(1.8,0.0)$. From the comparison between Figs. 1 and 2, it is clear that the core size of the constituent merons decreases when d increases, in agreement with Ref. 25. We find that both the distance between merons, $|z_L-z_R|$, and the core size of the merons decreases monotonically as d increases. We also find that for all values of $d<d_c$, the electron density projected in the $L(R)$ well is not even approximately circularly symmetric around $Z_{L(R)}$, and it has a minimum in $Z_{R(L)}$.

In Fig. 3, we plot the quasiparticle bimeron energy $\varepsilon_{\rm qp}$ as a function of d, for three different filling factors. Clearly an extrapolation to the dilute limit can be carried out reliably except possibly for very small d. For comparison, we also plot the single-particle quasiparticle energy. The energy of the bimeron is, for all values of d, smaller that the single-particle energy, in agreement with Ref. 25. (Both quasiparticle energies will be renormalized by quantum fluctuations neglected in the Hartree-Fock approximation.) For single-particle excitations, these corrections can be estimated by diagrammatic expansions,[36,6] and are not expected to be large. For pseudospin-texture quasiparticles, these corrections could be more important, as we comment further below, but are not likely to alter the energetic ordering obtained in our Hartree-Fock calculations. The filling factor dependence of the effective quasiparticle energy is largest at $d=0$ where the quasiparticle size is always limited by mutual interactions. At $d=0$, the quasiparticle energy should approach the ideal Skyrmion energy for quantum Hall ferro-

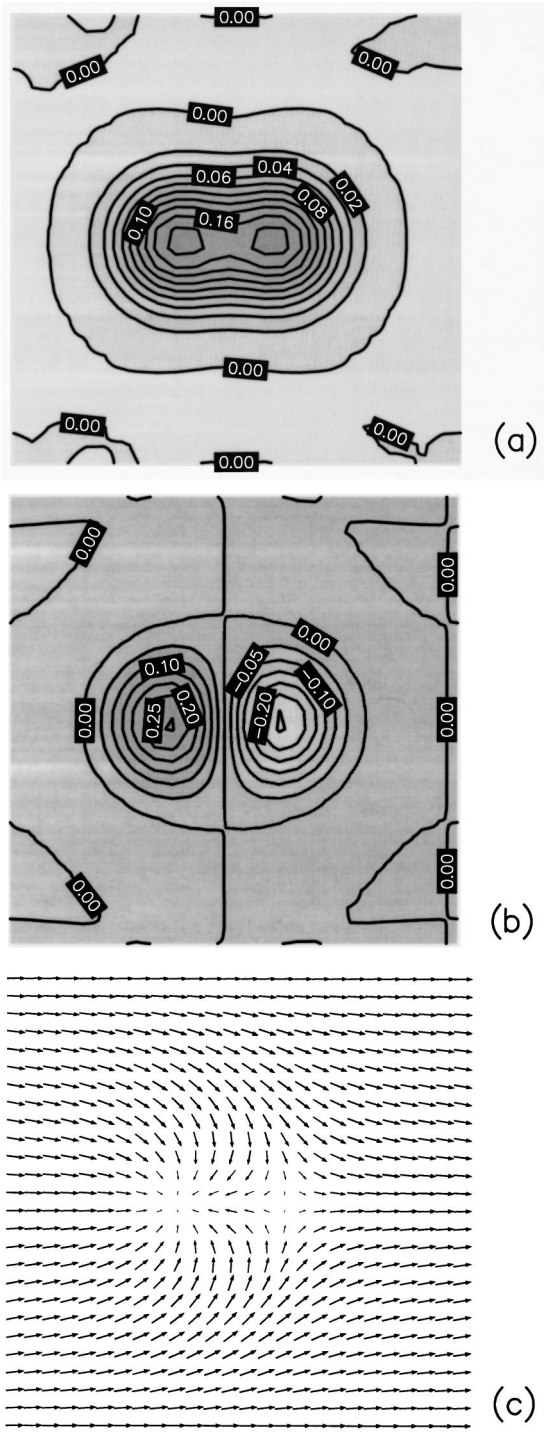

FIG. 2. (a) Excess of total charge density with respect to filling factor $\nu=1, n(\mathbf{r})-1/(2\pi\ell^2)$. (b) z component of the pseudospin density $S_z(\mathbf{r})$. (c) Two-dimensional vector representation of the x-y components of the pseudospin density for a bimeron in the cases $\nu=1.02, d=0.8$, and $t=0$. The figure corresponds to a square unit cell. In (a) and (b), the numerical values are given in units of $1/2\pi\ell^2$. In (c), the length of the arrows is proportional to the local magnitude of S_x and S_y, and their direction indicates the local orientation.

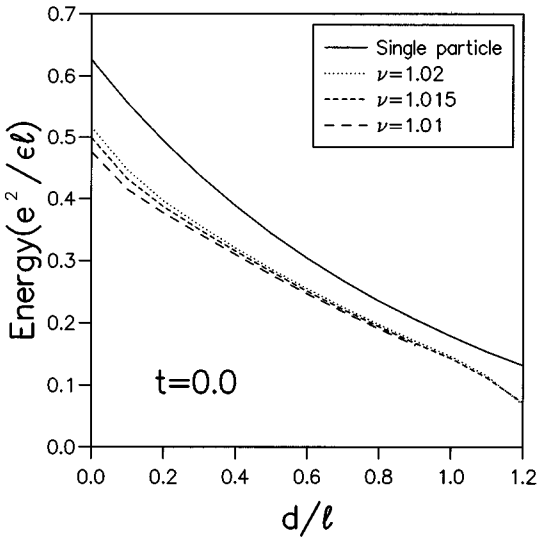

FIG. 3. Variation, as a function of d, of the quasiparticle bimeron energy, for three different filling factors. The single-particle HF quasiparticle energy is also shown.

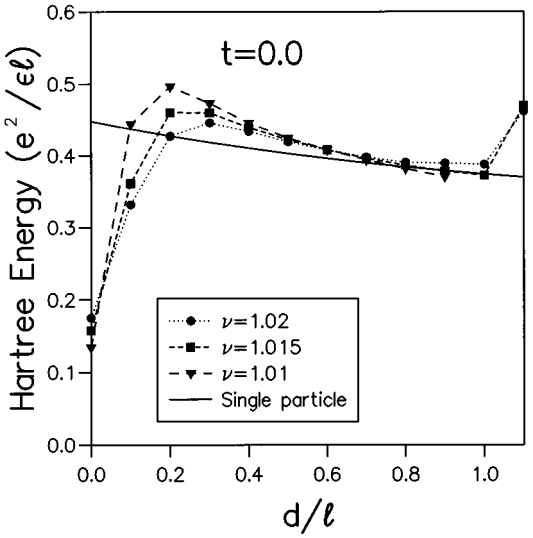

FIG. 5. Variation, as a function of d, of the Hartree contribution to the quasiparticle bimeron energy, for three different filling factors. The Hartree contribution to the single-particle HF quasiparticle energy is also shown.

magnets, $\sqrt{\pi/32}e^2/\epsilon\ell$.[13] When d increases, the dipolar term in Eq. (3) limits the meron core size, and the filling factor dependence of the effective quasiparticle energy eventually becomes negligible. For $d>0.5\ell$, we can describe the isolated bimeron limit rather accurately.

In Fig. 4, we show the dependence of $\langle S\rangle$ on d for different values of ν. Because of the variational character of the method of calculation, the bimeron size converges more slowly with ν than the energy. Nevertheless, it is clear from Fig. 4 that the bimeron decreases in size when d increases. At small $d(d<0.1\ell)$, the parameter $\langle S\rangle$ and other more detailed indices of the internal structure of the quasiparticle, do not change with d.

In Figs. 5 and 6, we plot, as a function of d, the Hartree and exchange contributions to the quasiparticle bimeron energy. For comparison, the values of these contributions to the quasiparticle energy in the single-particle HF case are also plotted. At small values of d $(d<0.25\ell)$, the Hartree quasiparticle energy increases with d. This is because at small d, in Eq. (3), the dipolar contribution to the Hartree energy grows faster than the capacitive contribution. At $d=0$, because of the presence of neighbors, the Hartree contribution to the quasiparticle energy is not zero, as expected in the case of an isolated Skyrmion. However, the numerical result obtained for the exchange contribution to the Skyrmion energy is very close to the ideal value $\sqrt{\pi/32}e^2/\epsilon\ell$.

In the Hartree-Fock approximation, the critical layer separation is reached when d reaches $d_c\sim 1.1\ell$. At this point, the easy-plane ferromagnet ground state at $\nu=1$ becomes unstable to the formation of charge-density waves. This is

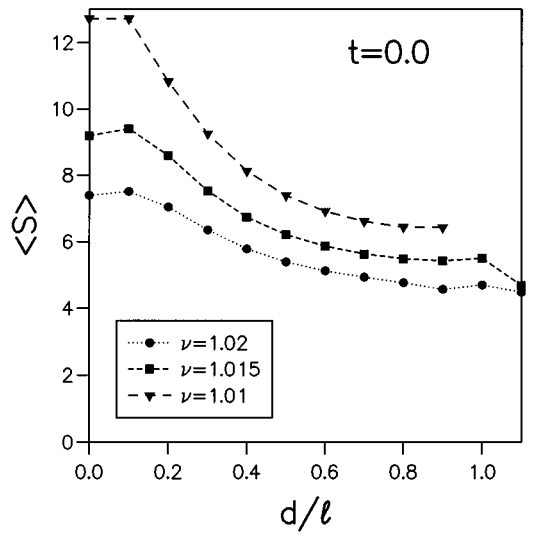

FIG. 4. Variation, as a function of d, of the quasiparticle parameter $\langle S\rangle$, for three different filling factors. In the case of the single-particle HF quasiparticle, $\langle S\rangle=1$.

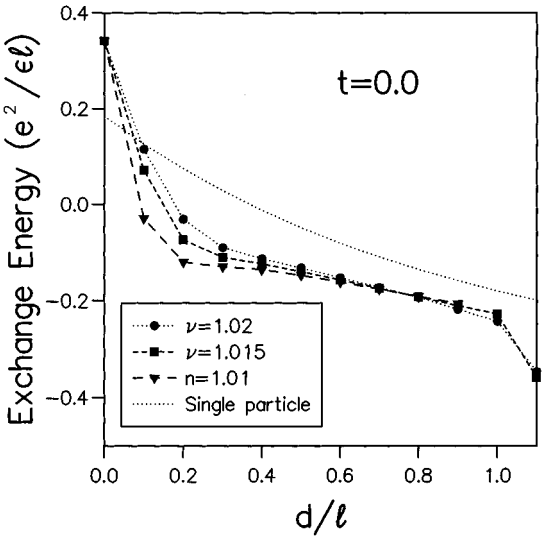

FIG. 6. Variation, as a function of d, of the exchange contribution to the quasiparticle bimeron energy, for three different filling factors. The exchange contribution to the single-particle HF quasiparticle energy is also shown.

reflected in our results in the fact that, for d larger than d_c the size of the quasiparticles diverges and the energy goes to zero. A related instability occurs in charged vortex effective models of double-layer systems.[37] However, in all likelihood, the charge-density-wave state we obtain at large d is an artifact of the Hartree-Fock approximation. Instead, the transition likely goes directly to a fluid state with weakly correlated compressible $\nu=\frac{1}{2}$ fluids[38] in each layer and no spontaneous coherence. Therefore, at $t=0$, the maximum value of d for which our calculations are reliable is $d=1.1\ell$, and due to the convergence of the results with respect to ν the minimum value is $d\sim 0.4\ell$.

Before finishing this subsection, we compare our results with those obtained using a field-theoretical approach by Yang and MacDonald.[25] These authors found that the distance between meron cores increases when d increases. Here we find the contrary; the bimeron decreases in size when d increases. For the quasiparticle energy, Yang and MacDonald found a energy just more than half of the result obtained here, and in better agreement with exact diagonalization studies.[6] The differences between our results and those of Ref. 25 are due to the neglect in that work of short-range repulsive interactions between the meron cores. In our calculations, there is no regime in which the bimeron can be treated as merons interacting only due to the gradient energy. We attribute differences between the values we obtain for the quasiparticle energy and estimates from exact diagonalization calculations[6] to quantum fluctuations that increases in importance as the layer separation increases. The quantum fluctuations renormalize the pseudospin stiffness and probably will also modify the energy and size of the bimerons. This effect will be more important for a larger layer separation d. If spontaneous coherence is lost with increasing layer separation via a continuous phase transition in which the pseudospin stiffness vanishes, there will be a regime close to the phase boundary where the bimeron size increases and the core size becomes relatively negligible. We can conclude from the present calculation that this regime will be quite narrow.

B. Tunneling amplitude different from zero

Figures 7 and 8 show the dependence of the quasiparticle energy and $\langle S\rangle$ on the tunneling gap $\Delta_{\rm SAS}=2t$. The bimeron quasiparticle energy increases with t because of the tunneling energy, and because the Hartree contribution to the quasiparticle energy increases when the size of the bimeron ($\sim\langle S\rangle$) decreases. Results are shown for $d=0.5\ell$ case; at this layer separation the effect of neighbors on the quasiparticle size is very small (see Figs. 3 and 4). The field theory estimates reviewed in Sec. III suggest that the bimeron should begin to shrink, and that the quasiparticle energy should begin to increase for $\Delta_{\rm SAS}>\Delta_{\rm SAS}^{\rm cr}$. For $d=0.5\ell$, the pseudospin stiffness in the x-y plane is $\rho_E\simeq 0.012e^2/\epsilon\ell$ and the crossover tunneling amplitude estimate given in Sec. III B is $\Delta_{\rm SAS}^{\rm cr}\sim 0.014e^2/\epsilon\ell$. Our numerical calculations give no indication of either an important crossover tunneling parameter or of a wide regime in which the quasiparticle energy is proportional to $t^{1/4}$ before finally crossing over to a single-particle regime with a contribution proportional to t. The field theory estimates fail to describe our calculations quantitatively because the dependence of the meron core energy on t contributes importantly to the tunneling amplitude dependence, and because the bimeron is not very large compared to either the meron core size or microscopic lengths. The change in curvature we find between the very large t regime where $\Delta\propto t$ and the stronger dependence at smaller values of t is qualitatively consistent with the field-theoretical predictions. The linear dependence of the charge gap on t at small t, which is probably most appropriately regarded as a core energy contribution, reflects the broken symmetry of the ground state. As mentioned above, the field theory estimates might be somewhat more successful in describing experiment than in describing our calculations since the spin stiffness which helps limit the meron separation in the bimeron is overestimated by the Hartree-Fock approximation, especially close to the critical layer separation.

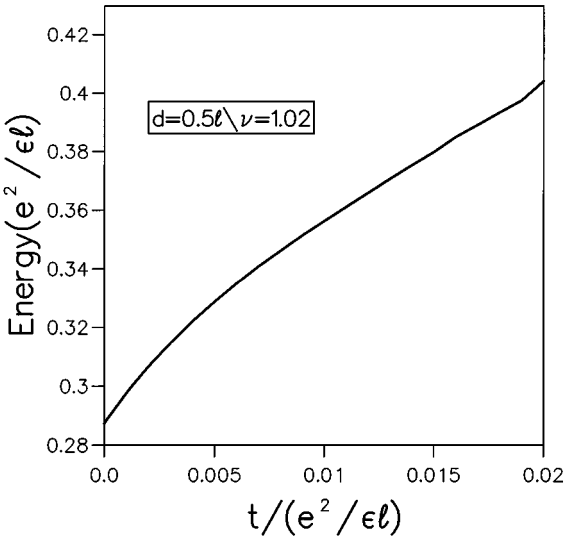

FIG. 7. Variation, as a function of t, of the quasiparticle bimeron energy, for $d=0.5\ell$ and $\nu=1.02$.

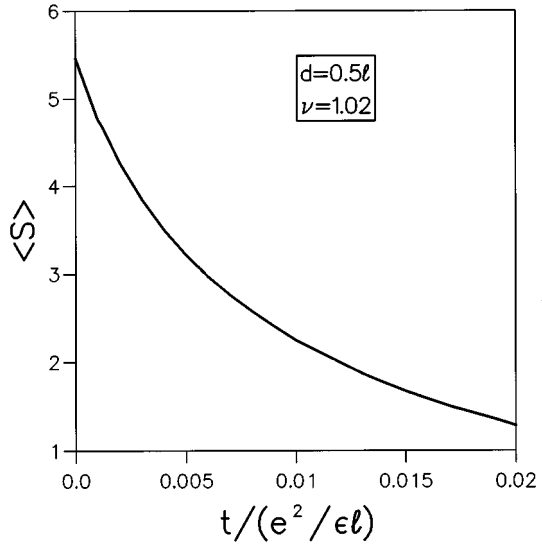

FIG. 8. Variation, as a function of t, of the quasiparticle parameter $\langle S\rangle$, for $d=0.5\ell$ and $\nu=1.02$. In the case of the single-particle HF quasiparticle, $\langle S\rangle=1$.

In Fig. 8, we observe that for $t \sim 0.02(e^2/\ell)$ the quasiparticle is close to a single-particle excitation with $\langle S \rangle = 1$. The tunneling parameter plays a role in this calculations similar to the role played by the Zeeman coupling in single-layer calculations. In both cases, the size of coupling required to recover single-particle excitations is surprisingly small.[14]

C. Effect of a parallel magnetic field

The inclusion of a parallel magnetic field $B_\parallel$ in the problem is responsible for the appearance of a length $\ell_\parallel$ in our calculations. In the commensurate phase, $B_\parallel$ destroys the translational invariance of the $\nu = 1$ ferromagnetic ground state, introducing in the system a periodicity $2\pi/Q$, with $Q = d/\ell^2$.

We study the dependence of the quasiparticle energies on parallel magnetic field by studying periodic structures with one extra electron per unit cell. We choose to work, as in previous sections, with a square lattice. The spatial variation of the hopping amplitude can be incorporated into our calculations without difficulty provided the lattice constant is an integer multiple of $2\pi/Q$. The results presented here were performed by choosing the density of charged excitations, so that this condition is satisfied. (For a square lattice, the lattice constant is $\sqrt{2\pi/|1-\nu|}\,\ell$ and for $B_\parallel$ applied in the $\hat{y}$ direction we choose ν so that this is an integer multiple of $2\pi/Q$.) The range of $B_\parallel$ which can be studied in this way is determined by the range of filling factors for which the form and size of the quasiparticle in the unit cell is not affected by the neighbors.

With this approach we are able to describe only the commensurate state and its charged excitations and the soliton lattice state with fixed period $2\pi/Q$ and its charged excitations. The incommensurate state is the strong parallel field limit of this soliton lattice state. The incommensurate state is never the true ground state, but closely approximates[32] the ground state on the large Q side of the transition, except for the region very close to Q_c where the solitons are widely spaced. In a parallel field, we find two separate self-consistent solutions to the Hartree-Fock calculations when no charged excitations are present (for $\nu = 1$) corresponding to the commensurate and soliton lattice states.

The energies of these two states are plotted a function of Q in Fig. 9 for $d = 0.5\ell$ and $t = 0.006e^2/\epsilon\ell$. The parallel field strength beyond which the soliton state has lower energy corresponds to $Q\ell = 0.37$, which should be compared with the field theory estimate $Q^*\ell = 0.36$. In Fig. 9, we also plot the energy per electron of the incommensurate state,

$$\varepsilon_0^I = -\tfrac{1}{4}[V_b(q=0) + V_d(q=0)]. \tag{31}$$

The energy per electron for the commensurate state is

$$\varepsilon_0^C = -t - \tfrac{1}{4}[V_b(q=0) + V_d(q=Q)]. \tag{32}$$

From Fig. 9, we see that the energies of the commensurate and incommensurate states cross at $Q_{C-I}\ell = 0.404$. Note that the soliton lattice has always lower energy than the incommensurate state.

When charged excitations are present we are able to find only one solution to the self-consistent Hartree-Fock equation at any value of Q. Spin textures for this state are illustrated in Fig. 10 for $Q\ell = 0.25$, and in Fig. 11 for $Q\ell = 0.5$. These illustrations demonstrate that the charged excitation changes from having the character of solutions found in the presence of hopping to having the character of solutions found without any hopping. We conclude from the smooth evolution of these solutions in our calculation, that the phase transition in a parallel field occurs only in a very narrow range around $\nu = 1$. Already for $\nu \sim 1.01$ there is no indication of a phase transition from the Hartree-Fock calculations, motivating further theoretical work to elucidate the physics which controls the dependence of the phase boundary on $|\nu - 1|$ and Q.

In Fig. 12, we present the resulting estimate of the dependence of the charge gap on parallel field. These estimates

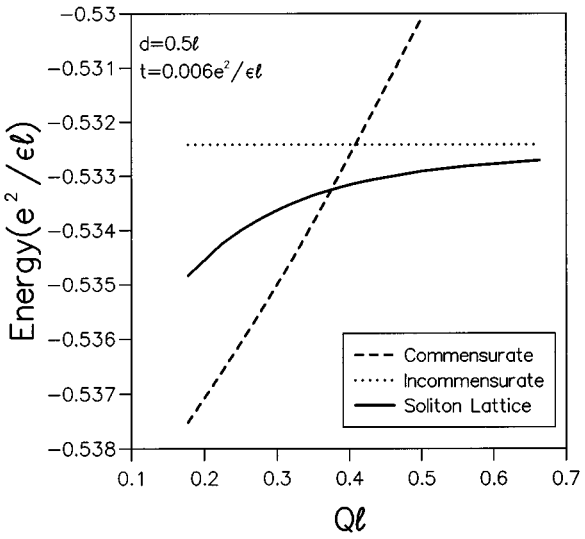

FIG. 9. Variation, as a function of $Q\ell$, of the energy per electron of the commensurate, incommensurate, and soliton lattice states at $\nu = 1$. The results correspond to the cases $d = 0.5\ell$ and $t = 0.006e^2/\epsilon\ell$.

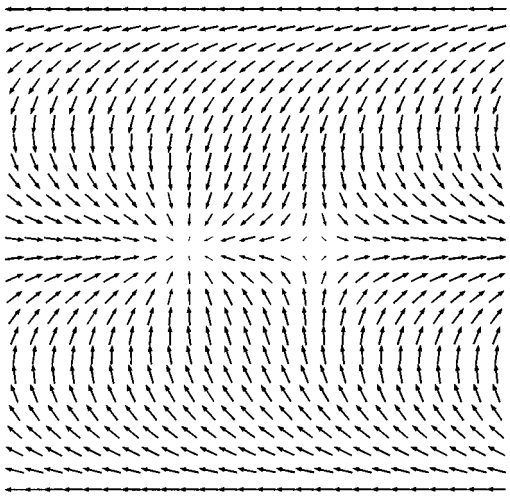

FIG. 10. Two-dimensional vector representation of the x-y components of the pseudospin density for a DQW system in the cases $d = 0.5\ell$, $t = 0.006e^2/\epsilon\ell$, and $Q\ell = 0.25$. The length of the arrows is proportional to the local magnitude of S_x and S_y, and their direction indicates the local orientation.

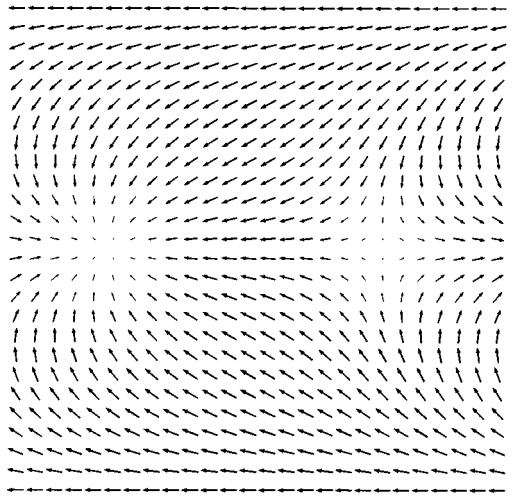

FIG. 11. Two-dimensional vector representation of the x-y components of the pseudospin density for a DQW system in the cases $d=0.5\ell$, $t=0.006e^2/\epsilon\ell$, and $Q\ell=0.50$. The length of the arrows is proportional to the local magnitude of S_x and S_y, and their direction indicates the local orientation.

have been improved by applying the Madelung energy correction for interactions between different charged excitations as explained in previous sections. In the range of filling factors for which these calculations have been done, we checked that we recovered previous estimates for the charge gap in the limits of zero parallel field and zero tunneling parameter. These illustrations demonstrate what we explained in previous sections. The cusp in this curve originates from the level crossing of the two ground-state energies. Our calculations *do not* provide useful information on the dependence of the charge gap very close to the phase transition, since in our soliton lattice state the distance between the soliton is fixed at $Q/2\pi$. In particular, the $\sim|Q-Q^*|^{1/2}$ predicted by Read could not be captured by our approach, although we believe that it does occur and could be captured by a more elaborate

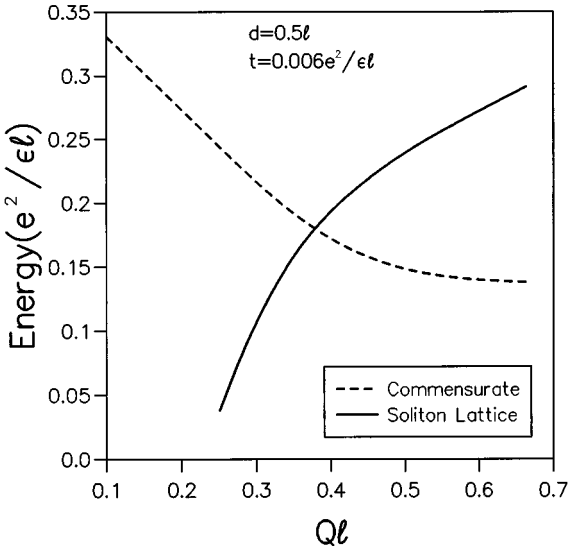

FIG. 12. Variation, as a function of $Q\ell$, of the quasiparticle energy with respect to the commensurate and soliton lattice phases. The results correspond to the cases $d=0.5\ell$ and $t=0.006e^2/\epsilon\ell$.

Hartree-Fock calculation. However, the large meron-core size and the large fraction of the charge gap provided by core energies means that the magnitude of the corresponding anomaly in the charge gap will be quite small, and that the domain-wall string picture of the charge excitation will apply only in a very narrow range of parallel fields around $Q=Q^*$. Away from this region, the only source of uncertainty in our calculations comes from the neglect of quantum fluctuations in the Hartree-Fock approximations.

For Q smaller than Q^*, the quasiparticle energy decreases with Q, because, in the commensurate phase, the pseudospin rotates in the x-y plane with a period proportional to Q^{-1}, and the gradient energy cost of creating a quasiparticle decreases when the rotation period increases. In the incommensurate phase, the pseudospin texture does not follow the parallel magnetic field, and the quasiparticle energy increases with Q until it reaches the value of the quasiparticle energy at $B_\parallel=0$ and $t=0$. The quasiparticle energy changes from $\varepsilon_{\rm qp}(d,t)$ at $B_\parallel$ to the value $\varepsilon_{\rm qp}(d,t=0)$ at infinite $B_\parallel$. Our calculations do not obtain a reduction in the quasiparticle energy as large as is found experimentally.[10] We think that the source of the disagreement is the neglect of quantum fluctuations in the Hartree-Fock approximation. These corrections will have a larger effect in reducing the charge gap in the incommensurate state, since tunneling is then not effective in their suppression.

VI. BIMERON AND MERON CRYSTALS

In this section, we comment on the rich possibilities for the ground state of a DQW system at filling factor near $\nu=1$, where the density of charged excitations is finite. We discuss some results we have obtained in the filling factors range $|\nu-1|<0.1$, where we believe the charged excitations are likely to crystallize, and the Hartree-Fock approximation is likely to be largely reliable.

Our results are obtained using the method described in Sec. IV, but some useful information can be obtained by considering possibilities using the field-theoretical language of Sec. II. In presence of N_e excess electrons with respect to $\nu=1$, the pseudospin unit vector $\mathbf{m}(\mathbf{r})$ can have the form of a N_e-order bimeron, specified by Eqs. (5) and (6):

$$w(z)=\prod_{i=1,N_e}\frac{z-z_{i,L}}{z-z_{i,R}}e^{i\varphi}. \tag{33}$$

This solution contains N_e pairs of merons with topological charge $\frac{1}{2}$ and opposite vorticities. In the pure ANLσM, the energies of the N_e-order bimeron does not depend on the location of the center of the merons $z_{i,L}$ and $z_{i,R}$, but depends *only* on the total topological charge N_e. However, since the topological charge density, Eq. (6), depends on the location of the meron centers, when other terms in Eq. (3) are taken into account, the energy of possible N_e-order bimeron states will depend on the locations of all meron centers. At zero temperature and at a filling factor close enough to $\nu=1$, we expect long-range Coulomb interactions to cause the meron centers to crystallize. The precise form of the pseudospin within each unit cell will depend on the filling factor, the tunneling amplitude, and the distance between layers.

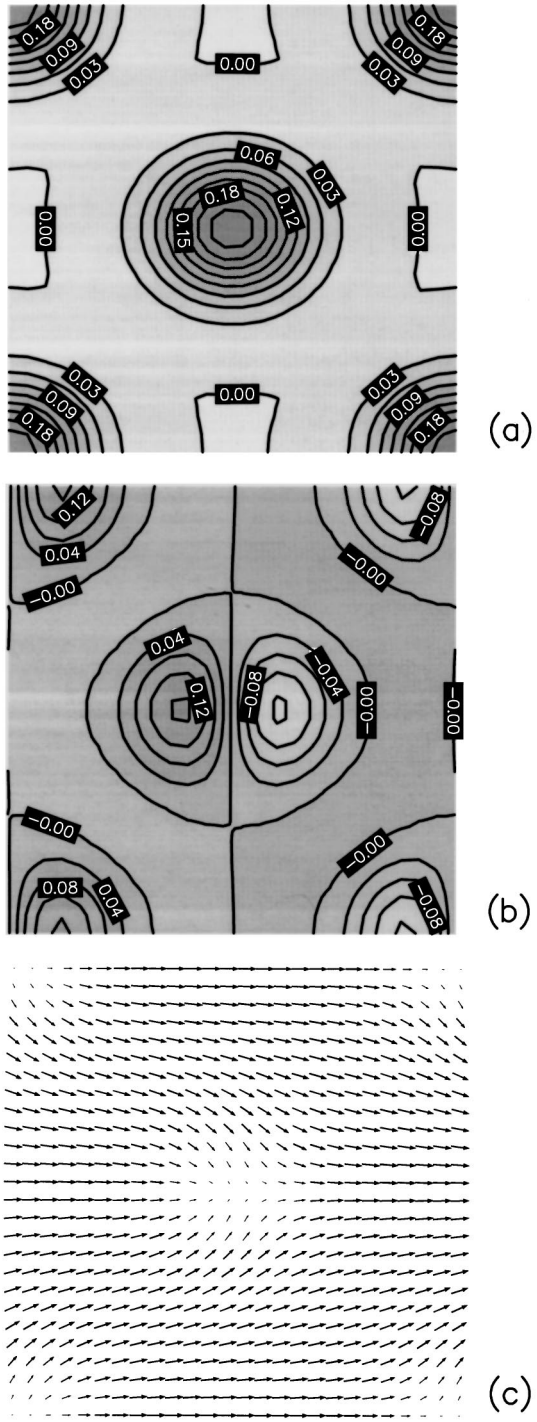

FIG. 13. (a) Excess of total charge density with respect to the filling factor $\nu=1, n(\mathbf{r})-1/(2\pi\ell^2)$. (b) z component of the pseudospin density $S_z(\mathbf{r})$. (c) Two-dimensional vector representation of the x-y components of the pseudospin density for a DQW system in the cases $\nu=1.04, d=0.8\ell$, and $t=0.01e^2/\epsilon\ell$. The figure corresponds to a square lattice with two extra electrons per unit cell with respect to $\nu=1$. In (a) and (b), the numerical values are given in units of $1/2\pi\ell^2$. In (c), the length of the arrows is proportional to the local magnitude of S_x and S_y, and their direction indicates the local orientation.

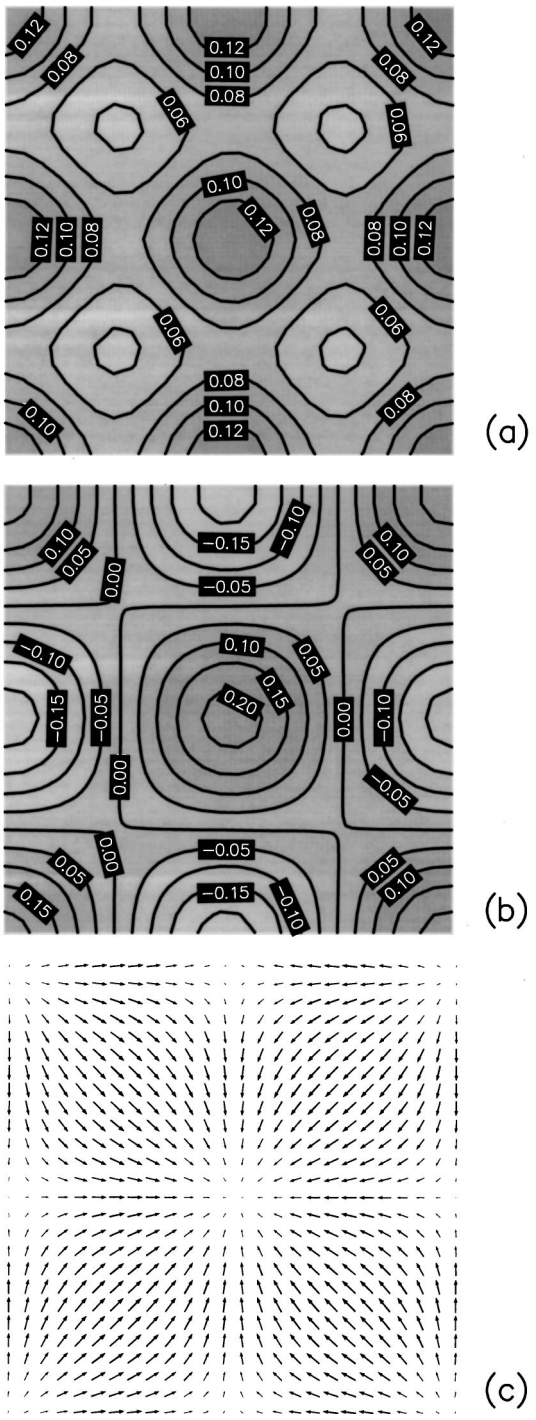

FIG. 14. (a) Excess of total charge density with respect to filling factor $\nu=1, n(\mathbf{r})-1/(2\pi\ell^2)$. (b) z component of the pseudospin density $S_z(\mathbf{r})$. (c) Two-dimensional vector representation of the x-y components of the pseudospin density for a DQW system in the cases $\nu=1.08, d=0.8\ell$, and $t=0$. The figure corresponds to a square lattice with two extra electrons per unit cell with respect to $\nu=1$. In (a) and (b), the numerical values are given in units of $1/2\pi\ell^2$. In (c), the length of the arrows is proportional to the local magnitude of S_x and S_y, and their direction indicates the local orientation.

Recently, we have found that the ground state of a 2DEG system at filling factor near $\nu=1$ is a Skyrme crystal.[21] For a Zeeman coupling different from zero ($\sim 0.015e^2/\epsilon\ell$), we found that the ground state is a square lattice Skyrme crystal with two Skyrmions per unit cell. When the Zeeman coupling decreases (~ 0) and the filling factor increases (~ 1.05), part of the charge density centered around the Skyrmions moves toward the interstitial region,[39] apparently

forming quasiparticles with topological charge $\frac{1}{2}$. And at a given ν, the ground state is a square lattice with four charged $e/2$ merons per unit cell. When the temperature increases, it has been proposed[40] that the ground state is a liquid of these charged $e/2$ quasiparticles.

In the DQW systems, at $t \neq 0$ and a filling factor close to $\nu=1$, we find that the ground state is a square-lattice bimeron crystal, with two bimerons per unit cell. Each bimeron is aligned along the $\hat{x}$ direction because of the tunneling energy. In one bimeron, the meron on the left has its core charge density in the left layer, and the meron on the right has its core charge in the right layer. For the other meron, this distribution is reversed. In Fig. 13, we plot the following numerical results for the case $d=0.8\ell$, $t=0.01e^2/\epsilon\ell$, and $\nu=1.04$: (a) the total charge density $n(\mathbf{r})$, (b) the z component of the pseudospin density $S_z(\mathbf{r})$ and, (c) the two-dimensional vector representation of the x-y components of the pseudospin density.

As the tunneling amplitude decreases and the filling factor increases, the bimeron charge starts to split more cleanly into two separate merons with charge $e/2$, until the ground state of the system eventually looks like a true meron crystal. The unit cell of this ground state is a square with four charged $e/2$ merons. In Fig. 14, we illustrate such a state for the cases $d=0.8\ell, t=0$, and $\nu=1.08$ by plotting (a) the total charge density $n(\mathbf{r})$, (b) the z component of the pseudospin density $S_z(\mathbf{r})$ and, (c) the two-dimensional vector representation of the x-y components of the pseudospin density. The pseudospin texture showed in Fig. 14 are well described by a function w,

$$w(z)=\lambda\sum_{n,m}\left[\frac{1}{z-R_{n,m}}-\frac{1}{z-R_{n,m}-R_{1,1}/2}\right], \qquad (34)$$

where λ is the meron size and $R_{n,m}$ are the lattice points: $R_{n,m}=nR_0+imR_0$, where R_0 is the lattice parameter. The minus sign in Eq. (34) corresponds to the rotation of one bimeron with respect to the other, as found in the Skyrme crystal. The poles of expression (34) correspond to the position of the merons with core charge in the left well. The zeros of Eq. (34) are located at $R_{n,m}+(R_0/2)$ and at $R_{n,m}+i(R_0/2)$, and they correspond to the position of the merons whose core charge is in the right well.

VII. SUMMARY

We used a superlattice approach to determine the nature of the charged excitations and the charge gap for double-layer quantum Hall systems at $\nu=1$ as a function of layer separation, tunneling amplitude between the layers, and tilt angles of the magnetic field away from the normal to the layers. This study was motivated by field-theoretical descriptions of the pseudospin texture charged excitations which occur at this filling factor because of spontaneous phase coherence in the incompressible ground state. If a pseudospin representation is used for the layer degree of freedom, the spontaneous phase coherence can be recognized as being equivalent to easy-plane ferromagnetic order. In the field theory description, the charged excitations consist of merons in the pseudospin field which carry charge $\pm e/2$, and are held together in pairs to form bimerons by forces which depend on the pseudospin stiffness and the tunneling amplitude between the two layers. Our microscopic Hartree-Fock calculations confirm many qualitative aspects of the field theory description of the elementary charged excitations in these systems. However, we find that the meron core sizes and the core contribution to the quasiparticle energies, which are most reliably estimated by microscopic calculations like those reported here, are large enough to invalidate quantitative aspects and some qualitative aspects of the field theory description. We have also explored the rich variety of crystalline states, including meron lattices and bimeron lattices, which we believe are the ground states of double-quantum-well systems for finite but small densities of charged excitations.

ACKNOWLEDGMENTS

We are grateful to C. Tejedor, L. M. Moreno, F. Guinea, J. P. Rodriguez, A. Somoza, S. M. Girvin, and Kun Yang for helpful discussions. This work was supported in part by NATO Collaborative Research Grant No. 930684, by the Comisión Interministerial de Ciencia y Tecnologia of Spain under Contract No. MAT 94-0982, and by the National Research Foundation under Grant Nos. DMR 94-16906 and DMR-9503814. H.A.F. acknowledges the support of the A. P. Sloan Foundation and the Research Corporation.

[1] See, for example, Y. W. Suen *et al.*, Phys. Rev. Lett. **68**, 1379 (1992); J. P. Eisenstein *et al.*, *ibid.* **68**, 1383 (1992).

[2] See, for example, B. I. Halperin, Helv. Phys. Acta **56**, 75 (1983); A. H. MacDonald, Surf. Sci. **229**, 1 (1990); Z. F. Ezawa and A. Iwazaki, Phys. Rev. B **47**, 7295 (1993); Song He *et al.*, *ibid.* **47**, 4394 (1983); T. Chakraborty and P. Pietilainen, Phys. Rev. Lett. **59**, 2784 (1987); E. H. Rezayi and F. D. M. Haldane, Bull. Am. Phys. Soc. **32**, 892 (1987); D. Yoshioka, A. H. MacDonald, and S. M. Girvin, Phys. Rev. B **39**, 1932 (1989).

[3] H. Fertig, Phys. Rev. B **40**, 1087 (1989); A. H. MacDonald *et al.*, Phys. Rev. Lett. **65**, 775 (1990); L. Brey, *ibid.* **65**, 903 (1990); X. M. Chen *et al.*, Phys. Rev. B **45**, 11 054 (1992); X. G. Wen and A. Zee, Phys. Rev. Lett. **69**, 1811 (1992); Z. F. Ezawa and A. Iwazaki, J. Mod. Phys. B **19**, 3205 (1992); Z. F. Ezawa (unpublished).

[4] We restrict our attention in this paper to balanced double-layer systems. For unbalanced external charges, broken symmetry states which have unequal densities in the two layers can still occur at $\nu=1$. See for example, T. Jungwirth and A. H. MacDonald, Phys. Rev. B **53**, 9943 (1996).

[5] R. Côté, L. Brey, and A. H. MacDonald, Phys. Rev. B **46**, 10 239 (1992); X. M. Chen and J. J. Quinn, *ibid.* **45**, 11 054 (1992).

[6] K. Moon *et al.*, Phys. Rev. B **51**, 5138 (1995).

[7] See, for example, A. H. MacDonald, in *Proceedings of the Les Houches Summer School on Mesoscopics Physics* (North-Holland, Amsterdam, 1995).

[8] G. S. Boebinger *et al.*, Phys. Rev. Lett. **64**, 1793 (1990).
[9] Y. W. Suen *et al.*, Phys. Rev. B **44**, 5947 (1991).
[10] S. Q. Murphy, J. P. Eisenstein, G. S. Boebinger, L. N. Pfeiffer, and K. W. West, Phys. Rev. Lett. **72**, 728 (1994).
[11] S. M. Girvin and A. H. MacDonald, in *Novel Quantum Liquids in Low-Dimensional Semiconductor Structures*, edited by S. Das Sarma and A. Pinczuk (Wiley, New York, 1995).
[12] R. Rajaraman, *Solitons and Instantons* (North-Holland, Amsterdam, 1982).
[13] S. L. Sondhi *et al.*, Phys. Rev. B **47**, 16 419 (1993).
[14] H. A. Fertig, L. Brey, R. Côté, and A. H. MacDonald, Phys. Rev. B **50**, 11 018 (1994).
[15] J. H. Oaknin *et al.*, Phys. Rev. B (to be published).
[16] E. H. Rezaty, Phys. Rev. B **36**, 5454 (1987); **43**, 5944 (1991).
[17] X. C. Xie and Song He, Phys. Rev. B **53**, 1046 (1996).
[18] S. E. Barret *et al.*, Phys. Rev. Lett. **74**, 5112 (1995).
[19] A. Schmeller *et al.*, Phys. Rev. Lett. **75**, 4290 (1995).
[20] E. H. Aifer, B. B. Goldberg, and D. A. Broido, Phys. Rev. Lett. **76**, 680 (1996).
[21] L. Brey, H. A. Fertig, R. Côté, and A. H. MacDonald, Phys. Rev. Lett. **75**, 2562 (1995).
[22] B. I. Halperin and P. C. Hohenberg, Phys. Rev. B **188**, 898 (1969).
[23] K. Yang *et al.*, Phys. Rev. Lett. **72**, 732 (1994).
[24] N. Read, Phys. Rev. B **52**, 1926 (1995).
[25] K. Yang and A. H. MacDonald, Phys. Rev. B **51**, 17 247 (1995).
[26] Eduardo Fradkin, *Field Theories of Condensed Matter Systems* (Addison-Wesley, Reading, MA, 1990).
[27] More precisely, the constant β has a contribution from capacitive charging energy and a contribution coming from the loss in exchange energy (Ref. 6).
[28] M. C. Ogilvie *et al.*, Nucl. Phys. B **190**, 325 (1981).
[29] T. Watanabe *et al.*, Prog. Theor. Phys. **65**, 164 (1981).
[30] A. A. Belavin and A. M. Poliakov, Pis'ma Zh. Éksp. Teor. Fiz. **22**, 503 (1975) [JETP Lett. **22**, 245 (1975)].
[31] See Fig. 11 in *Novel Quantum Liquids in Low-Dimensional Semiconductor Structures* (Ref. 11).
[32] R. Côté, L. Brey, H. Fertig, and A. H. MacDonald, Phys. Rev. B **51**, 13 475 (1995).
[33] R. Morf and B. I. Halperin, Phys. Rev. B **33**, 2221 (1986).
[34] A. H. MacDonald and S. M. Girvin, Phys. Rev. B **34**, 5639 (1986).
[35] L. Bonsall and A. A. Maradudin, Phys. Rev. B **15**, 1959 (1977).
[36] Luis Brey, Phys. Rev. B **47**, 4585 (1993).
[37] I. Tupitsyn, M. Wallin, and A. Rosengren, Phys. Rev. B **53**, R7614 (1996).
[38] B. I. Halperin, P. A. Lee, and N. Read, Phys. Rev. B **47**, 7312 (1993).
[39] L. Brey, H. A. Fertig, R. Côté, and A. H. MacDonald, Phys. Scr. (to be published).
[40] A. G. Green, I. I. Kogan, and A. M. Tsvelik, Phys. Rev. B **53**, 6981 (1996).